REGULAR ARTICLE

blood advances

AMG 701 induces cytotoxicity of multiple myeloma cells and depletes plasma cells in cynomolgus monkeys

Rebecca L. Goldstein,[1,*] Ana Goyos,[1,*] Chi-Ming Li,[1] Petra Deegen,[2] Pamela Bogner,[2] Alexander Sternjak,[2] Oliver Thomas,[2] Matthias Klinger,[2] Joachim Wahl,[2] Matthias Friedrich,[2] Benno Rattel,[2] Edwin Lamas,[3] Xiaoshan Min,[1] Athena Sudom,[1] Mozhgan Farshbaf,[1] Angela Coxon,[3] Mercedesz Balazs,[1,†] and Tara Arvedson[1,†]

[1]Amgen Research, Amgen Inc., South San Francisco, CA; [2]Amgen Research (Munich) GmbH, Munich, Germany; and [3]Amgen Research, Amgen Inc., Thousand Oaks, CA

Key Points

- AMG 701 induced T-cell–dependent cellular cytotoxicity of BCMA-expressing target cells, which was augmented by PD-1 blockade.
- In vivo, AMG 701 prolonged survival of tumor-bearing mice and depleted PCs in cynomolgus monkeys.

Multiple myeloma (MM) is a hematologic malignancy that is characterized by the accumulation of abnormal plasma cells (PCs) in the bone marrow (BM). Patient outcome may be improved with BiTE (bispecific T-cell engager) molecules, which redirect T cells to lyse tumor cells. B-cell maturation antigen (BCMA) supports PC survival and is highly expressed on MM cells. A half-life extended anti-BCMA BiTE molecule (AMG 701) induced selective cytotoxicity against BCMA-expressing MM cells (average half-maximal effective concentration, 18.8 ± 14.8 pM), T-cell activation, and cytokine release in vitro. In a subcutaneous mouse xenograft model, at all doses tested, AMG 701 completely inhibited tumor formation ($P < .001$), as well as inhibited growth of established tumors ($P \leq .001$) and extended survival in an orthotopic MM model ($P \leq .01$). To evaluate AMG 701 bioactivity in cynomolgus monkeys, a PC surface phenotype and specific genes were defined to enable a quantitative digital droplet polymerase chain reaction assay (sensitivity, 0.1%). Dose-dependent pharmacokinetic and pharmacodynamic behavior was observed, with depletion of PC-specific genes reaching 93% in blood and 85% in BM. Combination with a programmed cell death protein 1 (PD-1)–blocking antibody significantly increased AMG 701 potency in vitro. A model of AMG 701 binding to BCMA and CD3 indicates that the distance between the T-cell and target cell membranes (ie, the immunological synapse) is similar to that of the major histocompatibility complex class I molecule binding to a T-cell receptor and suggests that the synapse would not be disrupted by the half-life extending Fc domain. These data support the clinical development of AMG 701.

Introduction

Multiple myeloma (MM), a clonal proliferation of malignant plasma cells (PCs) in the bone marrow (BM),[1] accounts for ~17% of the hematologic malignancies in the United States.[2,3] Despite recent advances in the treatment of MM, there are no curative therapies, and relapse is expected.[1] Approximately half of patients survive for 5 years after diagnosis,[3] highlighting the urgent need for novel therapeutic treatments for MM.

Immunotherapy is a promising approach for MM treatment. One strategy is to redirect a patient's own T cells to eliminate cancer cells using BiTE (bispecific T-cell engager) molecules, which bind the T-cell

Submitted 4 June 2020; accepted 31 July 2020; published online 4 September 2020.
DOI 10.1182/bloodadvances.2020002565.

*R.L.G. and A.G. contributed equally to this work.

†M.B. and T.A. contributed equally to this work.

Data sharing requests should be sent to Tara Arvedson (taraa@amgen.com). Qualified researchers may request data from Amgen clinical studies. Complete details are available at the following: https://wwwext.amgen.com/science/clinical-trials/clinical-data-transparency-practices/.

The full-text version of this article contains a data supplement.

receptor (TCR)-associated CD3ε protein and a tumor-associated antigen. BiTE molecules mediate the interaction of T cells with cancer cells, leading to the formation of an immunological synapse, T-cell activation, cytokine secretion, and target cell apoptosis.[4] The CD19-targeting BiTE molecule blinatumomab is the first bispecific T-cell–engaging therapy to be approved by the US Food and Drug Administration (FDA) for treatment of minimal residual disease–positive and relapsed or refractory B-cell precursor acute lymphoblastic leukemia.[5,6]

B-cell maturation antigen (BCMA), a transmembrane protein belonging to the tumor necrosis factor receptor super family, plays a central role in regulating B-cell maturation and differentiation into PCs.[7] BCMA is an attractive target for MM immunotherapy because of its high expression on malignant PCs in MM patients and normal expression restricted to PCs in healthy individuals.[8,9] BCMA-targeting therapeutics in clinical development include BCMA-targeting antibody-drug conjugates,[9-13] BCMA-specific chimeric antigen receptor T-cell therapies,[14-19] and BCMA-targeting bispecific antibodies.[20,21] Many of these therapeutics have demonstrated promising antimyeloma activity in nonclinical and early-phase clinical studies. The advantages of the BiTE molecule modality include potent mechanism of action and off-the-shelf utility, warranting evaluation in MM.

AMG 420 is a BiTE molecule directed against BCMA that induces selective T-cell–dependent cellular cytotoxicity (TDCC) against BCMA-expressing cells in vitro and in vivo.[20] In a phase 1 first-in-human (FIH) study in relapsed and/or refractory MM patients (NCT02514239), AMG 420 demonstrated a 70% objective response rate at the dose of 400 μg/d, providing the first clinical proof of concept for BiTE molecule therapy in MM.[22] AMG 420 has a short in vivo half-life, necessitating continuous IV infusion to maintain drug exposure in patients.[22] The aim of this study was to generate and evaluate preclinically a half-life extended (HLE) anti-BCMA BiTE molecule (AMG 701) as a therapy for MM. AMG 701 is being examined in a phase 1 FIH dose-finding study in relapsed/refractory MM patients (NCT03287908).

Methods

Animal welfare

All in vivo work was conducted under protocols that were approved by the Institutional Animal Care and Use Committee in Association for Assessment and Accreditation of Laboratory Animal Care–accredited facilities. Animal experimental procedures were conducted in accordance with the German Animal Welfare Law, with permission from the responsible local authorities, and within the guidelines of the Association for Assessment and Accreditation of Laboratory Animal Care international standards. Cynomolgus monkeys were cared for in accordance with the Guide for the Care and Use of Laboratory Animals, eighth edition.

Cell lines

Cell lines analyzed were sourced from commercial vendors and cultured according to the vendors' specifications.

Quantitation of BCMA surface protein expression on target cell lines

BCMA surface molecule quantitation on cancer cell lines was determined using QIFIKIT (Dako; cat. no. K0078) with anti-BCMA antibody 9C2H4 (Boehringer Ingelheim) or an internal clone (Amgen Research [Munich] GmbH).

TDCC assay and T-cell activation

Flow-based TDCC. BCMA$^+$ or BCMA$^-$ target cells were labeled with Vybrant DiO or DiI fluorescent dyes (Invitrogen; cat no. V22885 and V22886). Human peripheral blood mononuclear cells (PBMCs; Institute for Clinical Transfusion Medicine and Immunogenetics, University of Ulm, Ulm, Germany) and cynomolgus monkey effector cells (PBMCs and T cells isolated therefrom; R.C. Hartelust, BV, Tilburg, The Netherlands) were cocultured with target cells at a 10:1 ratio and increasing concentrations of AMG 701 for 48 hours. Target cell lysis was monitored by flow cytometric determination of propidium iodide uptake by target cells and the upregulation of CD25 and CD69 on CD4$^+$ and CD8$^+$ T cells by flow cytometry (BD FACSCanto II and fluorescently labeled antibodies; BD Biosciences). For TDCC assays utilizing KMS12BM_PDL1 and U266B1_PDL1 GFP$^+$ target cells, remaining viable target cells (GFP$^+$ ToPro3$^-$) were enumerated by flow cytometry.

Programmed cell death protein 1 (PD-1) expression was measured on T cells (Figure 6A) by flow cytometry (BD FACSymphony Flow Cytometer; BD Biosciences) utilizing an antibody cocktail (supplemental Table 5). For TDCC assays utilizing PD-1$^+$ T cells, human pan T cells were preincubated 1:1 with CD3/CD28 Dynabeads (Thermo Fisher) for 48 hours.

Cytokine release

Cytokine levels in the supernatants of flow-based TDCC assays were analyzed by human and nonhuman primate Th1/Th2 cytometric bead arrays (BD Biosciences), according to the manufacturer's instructions. Cytokine levels (Figure 6E) were measured from supernatants collected at 72 hours of the TDCC assay (Figure 6D), using an enzyme-linked immunosorbent assay (Meso Scale Discovery).

Mouse xenograft models

Flank model. NCI-H929 MM cells mixed with human PBMCs (effector-to-target [E:T]: 1:2) were injected subcutaneously into the right flank of sublethally irradiated female nonobese diabetic (NOD)/severe combined immunodeficiency (SCID) mice. Before tumors were measurable, mice were treated with vehicle or AMG 701 (2, 0.2, and 0.02 mg/kg) by IV bolus injection into the lateral tail vein on days 3, 8, and 13. Tumor growth was measured 2 or 3 times per week using calipers. Statistical significance was calculated using 1-way analysis of variance (ANOVA) with the Dunnett post hoc test.

Aggressive model. Sublethally irradiated NOD/SCID mice were injected IV with 1×10^7 L-363 MM tumor cells on day 1. On day 4, all mice (with the exception of vehicle-only control group) received a single IV dose of anti–asialo GM1 antibody (Cedarlane/BIOZOL, cat. no. CL8955; Lot TGP5888) into the lateral tail vein to deplete the remaining natural killer cells. A total of 2×10^7 in vitro expanded human CD3$^+$ T cells (human T Cell Isolation Kit and T Cell Activation/Expansion Kit, human; Miltenyi Biotec) were injected into the peritoneal cavity of all mice, with the exception of the vehicle-only control group, on day 5. Mice were treated with AMG 701 (0.5, 0.05, and 0.005 mg/kg) or vehicle on day 9, and then every 5 days for 6 administrations, and were monitored daily.

Statistical significance of the survival benefit was calculated using a log-rank (Mantel-Cox) test.

Established model. On day 1, 5×10^6 NCI-H929 MM cells were injected subcutaneously into the right flank of sublethally irradiated female SCID mice. On day 8, 1.2×10^7 human T cells were injected intraperitoneally into all animals. Mice were treated with vehicle or AMG 701 (0.25, 0.05, or 0.01 mg/kg) on day 15 and day 22 and were monitored daily. Statistical significance was calculated using 1-way ANOVA with the Dunnett post hoc test.

Pharmacokinetics in cynomolgus monkeys

AMG 701 was quantified by a ligand-binding assay based on electrochemiluminescent technology (Meso Scale Discovery). All samples were analyzed by a generic approach: an antibody directed against the CD3-binding portion of the BiTE antibody construct was used as coating reagent, and a noncompeting anti-CD3–binding ruthenium-labeled antibody was used for detection. Pharmacokinetics (PK) parameters were fitted with Phoenix WinNonlin software using noncompartmental analysis.

Immunophenotyping

Cynomolgus macaque (Chinese) whole blood (Valley Biosystems, Alameda, CA), collected into Na/heparin within 4 hours of blood draw, was stained by adding 2.5 μL of mouse serum to each well of a U-bottom 96-well plate, followed by the addition of 100 μL of blood and then fluorochrome-labeled antibody cocktail (supplemental Table 4). Blood was then lysed with BD Pharm Lyse. From each sample, 250 000 cells were collected and analyzed on a BD LSR II Flow Cytometer. Geometric median fluorescence intensity was determined from each sample for each population using FlowJo software.

Bone marrow mononuclear cells (BMMCs) were isolated from fresh cynomolgus monkey BM aspirate (Alpha Genesis) by separation over Lympholyte-Mammal Cell Separation Media (CEDARLANE). Cells were stained with fluorochrome-labeled antibody cocktail (supplemental Table 5). For intracellular staining, after cell surface staining, cells were permeabilized with BD Cytofix/Cytoperm (BD Biosciences), washed with BD Perm/Wash buffer (BD Biosciences), and stained with anti-p63 (FITC Mouse Anti-Human p63; clone VS38), and anti–immunoglobulin M (IgM) [AffiniPure PE Goat Anti-Human IgM $F(ab')_2$ $Fc_{5\mu}$ fragment specific; Jackson ImmunoResearch Laboratories]. For staining of human PCs, human BM (AllCells) was stained with a fluorochrome-labeled antibody cocktail (supplemental Table 5). For analysis, doublets were gated out, and dead cells were excluded by 7-aminoactinomycin D. Cells were analyzed using a BD LSR II Flow Cytometer and FlowJo software.

Pharmacodynamics/ddPCR assays for cynomolgus monkey studies

Complementary DNA was generated from RNA isolated from blood and BM. Reaction mixes for droplet digital polymerase chain reaction (ddPCR) were prepared using Bio-Rad's ddPCR Supermix for Probes kit (cat. no. 1863010) and custom-designed Integrated DNA Technologies' PrimeTime qPCR Probe Assays (sequences in supplemental Methods). Reaction droplets were generated, and the recommended thermal cycling conditions were carried out on a Bio-Rad C1000 Touch thermal cycler. The 40-μL reactions were measured on the QX100 or QX200 droplet reader. Instrument readouts were generated as the number of copies per microliter and then converted to copies per nanogram, based on the complementary DNA input.

Results

AMG 701 induced potent and specific TDCC against MM cell lines in vitro

A panel of BCMA protein-positive or -negative target cell lines (Figure 1A; supplemental Table 1) was used to evaluate AMG 701 TDCC activity in vitro. AMG 701 induced potent TDCC in cocultures of human PBMCs with 4 BCMA protein-positive MM cell lines, with half-maximal effective concentration (EC_{50}) values ranging from 0.8 ± 1.0 pM to 42.0 ± 25.3 pM (mean ± SD, n = 4-6 PBMC donors per cell line; average EC_{50}, 18.8 ± 14.8 pM; Figure 1B; supplemental Table 1), but not with BCMA protein-negative HCT-116 cells, demonstrating the selectivity of AMG 701. In the presence of BCMA cell surface–positive cells, but not BCMA cell surface–negative cells, AMG 701 induced dose-dependent T-cell activation (Figure 1C-D) and dose- and time-dependent cytokine secretion (Figure 1E).

AMG 701 has comparable intraspecies binding affinity for BCMA and CD3 in human and cynomolgus monkey (supplemental Table 2). Using cynomolgus monkey effector cells, AMG 701 induced potent and specific TDCC of BCMA cell surface–expressing cells (supplemental Figure 1A), T-cell activation (supplemental Figure 1B-C), and cytokine secretion (supplemental Figure 1D-E).

AMG 701 demonstrated antitumor activity in mouse xenograft models

AMG 701 was evaluated in vivo in an MM mouse xenograft flank model. NCI-H929 BCMA protein-positive MM cells mixed with human PBMCs at an E:T ratio of 1:2 were injected subcutaneously into sublethally irradiated NOD/SCID mice. Treatment with AMG 701 began on day 3, when tumors were not measurable. Tumor volume measurement began on day 6 (40-65 mm^3 across all groups). Complete inhibition of tumor formation was observed at all 3 doses tested (0.02, 0.2, and 2 mg/kg; $P < .001$; Figure 2A). Serum exposures were dose dependent (Figure 2B), with resulting elimination half-lives ($t_{1/2}$) of 170, 153, and 90 hours, respectively. AMG 701 was well tolerated, as evidenced by no body weight loss.

An aggressive orthotopic MM mouse model (L-363 MM cells) was used to further evaluate AMG 701 in vivo. Despite the highly aggressive nature of this model, treatment with AMG 701 extended survival significantly at all doses tested compared with controls (Figure 2C; $P = .007$ [0.005 mg/kg], $P < .001$ [0.05 and 0.5 mg/kg]; Kaplan-Meier estimator with Mantel-Cox log rank). In the aggressive L-363 model, body weight loss occurred in some mice 2 to 5 days before death because of disease progression, and this observation was deemed irrelevant to treatment, because AMG 701 does not bind murine BCMA.

AMG 701 was further evaluated in an established MM mouse model. NCI-929 MM cells were injected subcutaneously into

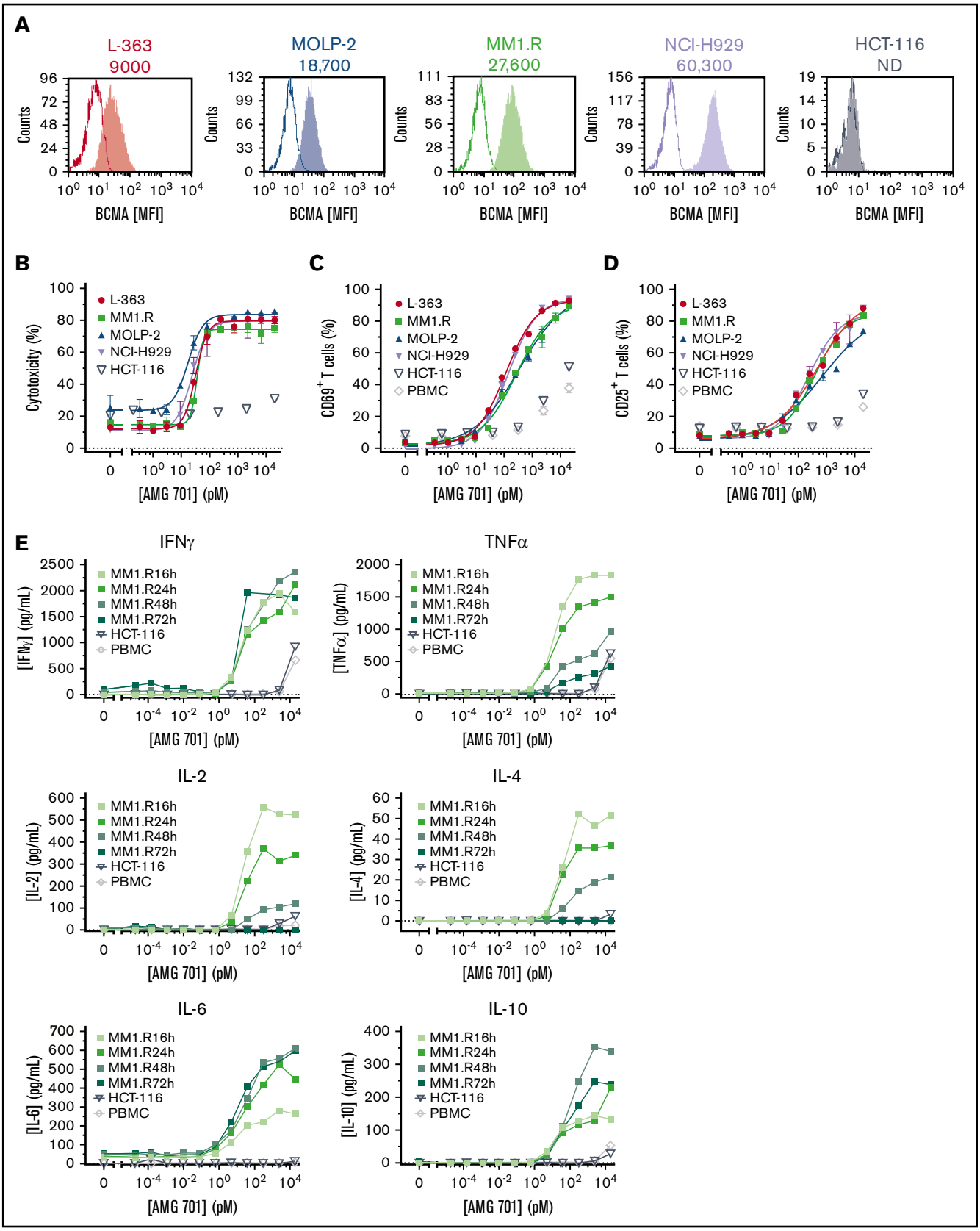

Figure 1. AMG 701 induced TDCC against MM cell lines in vitro. (A) Flow cytometry histograms depicting BCMA cell surface protein expression on cancer cell lines. Open graphs represent isotype staining; filled graphs represent BCMA protein staining. Numbers represent the number of BCMA molecules per cell. (B) Specific cytotoxicity

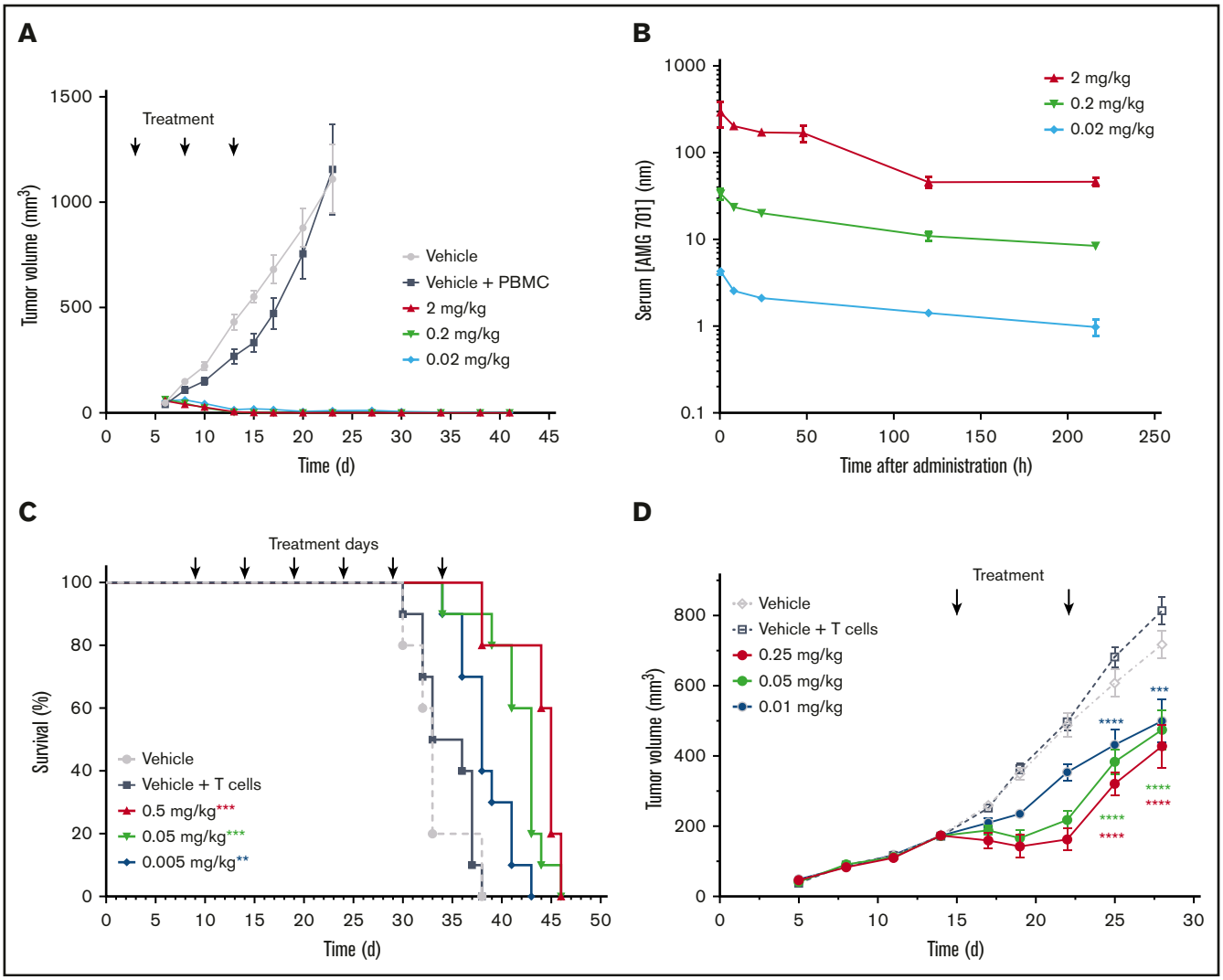

Figure 2. AMG 701 demonstrated antitumor activity in mouse xenograft models. (A) Tumor volumes of NOD/SCID mice injected subcutaneously with a mixture of NCI-H929 tumor cells and human PBMCs (1:2 E:T ratio) and treated with vehicle or AMG 701 (2, 0.2, and 0.02 mg/kg) on days 3, 8, and 13. Data are mean ± standard error of the mean (SEM) (n = 5, vehicle group; n = 10, all other groups). $P < .001$ for all dose levels from day 10 until day 23 vs vehicle + PBMC group, 1-way ANOVA with the Dunnett post hoc test. (B) PK profile of AMG 701 in mouse serum at the times indicated after the last administration on day 13. Data are mean ± SEM (n = 3). (C) Kaplan-Meier survival analysis of NOD/SCID mice orthotopically transplanted with L-363 MM cells, injected intraperitoneally with human T cells on day 5 (except for vehicle-only control), and treated with AMG 701 (0.5, 0.05, and 0.005 mg/kg) or vehicle every 5 days for 6 administrations, starting on day 9. Arrows indicate days of treatment (n = 5, vehicle group; n = 10, all other groups). $^{**}P = .007$, $^{***}P < .001$ vs vehicle + T-cell group, Kaplan-Meier estimator with Mantel-Cox log-rank test. (D) Tumor volumes of SCID mice injected subcutaneously with NCI-H929 tumor cells (5E6) on day 1, intraperitoneally injected with human T cells (1.2E7) on day 8, and treated with vehicle or AMG 701 (0.25, 0.05, or 0.01 mg/kg) on days 15 and 22. Data are mean ± SEM (n = 5, vehicle group; n = 8, all other groups). $^{****}P < .0001$, $^{***}P = .0002$, 1-way ANOVA with the Dunnett post hoc test.

sublethally irradiated SCID mice, followed by intraperitoneal injection of human T cells 1 week later. On day 15, tumor volume averaged 173.2 ± 22.1 mm^3, and treatment with AMG 701 began. After 2 treatments, on day 28, AMG 701 inhibited tumor growth at all 3 doses tested (Figure 2D; $P < .0001$ [0.25 and 0.05 mg/kg]; $P = .0002$ [0.01 mg/kg]).

Figure 1. (continued) of TDCC assays with BCMA protein-positive cell lines (L-363, MM1.R, MOLP-2, NCI-H929) or the BCMA protein-negative cell line (HCT-116) cocultured with human PBMCs at a 5:1 E:T ratio and increasing concentrations of AMG 701 for 48 hours. Data are mean ± standard deviation (SD) for 2 technical replicates. Curves are representative of 4 PBMC donors. Expression of CD69 (C) and CD25 (D) on T cells from TDCC assays of $BCMA^+$ or $BCMA^-$ cell lines or no target cells (PBMC), as described in panel B. Data are mean ± SD of 2 technical replicates representative of 4 PBMC donors. (E) Concentration of cytokines in supernatants of TDCC assays at the times indicated. Data represent 1 technical replicate from 1 PBMC donor. IFNγ, interferon-γ; IL-2, interleukin-2; MFI, mean fluorescence intensity; ND, not detectable; TNFα, tumor necrosis factor-α.

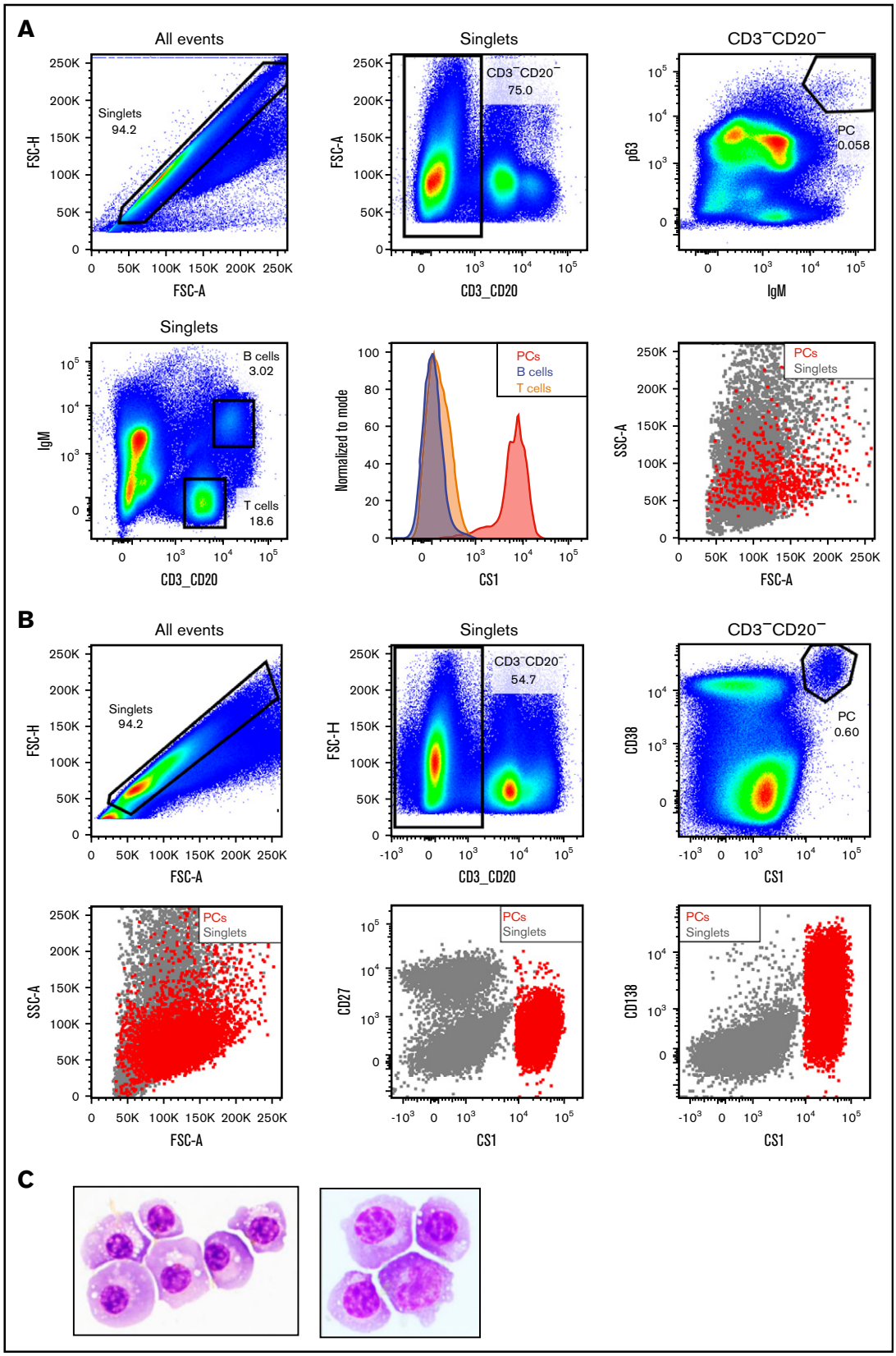

Figure 3. Identification of cynomolgus monkey plasma cell surface phenotype allows cell sorting. (A) Intracellular and cell surface flow cytometry analysis of cynomolgus monkey BM. PCs: $CD3^{-}CD20^{-}$ singlets positive for intracellular p63 and IgM (upper panels). Gating strategy to identify BM T and B lineage cells in cynomolgus monkey BM (lower left panel). Flow cytometry graphs depicting CS1 expression on PCs (red), T cells (orange), and B cells (steel blue) from cynomolgus monkey BM (lower

Identification of cynomolgus monkey PC surface phenotype

To further characterize AMG 701, a study of the PK/pharmacodynamics (PD) relationship in cynomolgus monkeys was performed. Based on species similarity to humans, cynomolgus monkey PCs were anticipated to be the target of BiTE molecule–redirected lysis; however, quantitation of AMG 701–mediated depletion of PCs by flow cytometry is challenging because cytometry-based measurement of very rare cells, such as PCs (0.1%-3% of BMMCs or PBMCs),[23-25] is unreliable.[26,27] To address these limitations, a sensitive and quantitative ddPCR-based assay was developed to measure PC depletion in vivo. At the time of this study, a defined cell surface phenotype of cynomolgus monkey PCs was not available. A pure population of putative cynomolgus monkey BM PCs was isolated using the known PC intracellular proteins IgM and p63. The isolated cells were large lymphocytes with intermediate scatter properties, exhibiting characteristic morphological features of PCs (Figure 3A). Similar to human PCs,[28-32] these cells expressed high levels of cell surface CS1 and CD38 and showed heterogeneous expression of CD138 protein, but not CD27, unlike human PCs[29,30] (Figure 3A-B; supplemental Figure 2). The IgM^+ $p63^+$ cells were subsequently confirmed as PCs by Wright Giemsa staining and morphological analysis of cytospin preparations (Figure 3C). Based on this work, the cell surface phenotype of cynomolgus monkey PCs was determined to be $CD3^{neg}CD20^{neg}$ $CS1^{hi}CD38^{hi}CD138^{het}CD27^{neg}$.

BCMA is expressed on human and cynomolgus monkey PCs but not B cells

Cell surface BCMA protein expression on cynomolgus monkey PCs was subsequently evaluated and compared with that of BM-derived and circulating B cells. Because commercially available antibodies exhibited poor reactivity to cynomolgus monkey BCMA, a monoclonal anti-BCMA antibody (P62682.3) was generated. This antibody was subsequently biotinylated, confirmed active (supplemental Figure 3A-B), and used to evaluate BCMA surface expression on cynomolgus monkey BM-derived PCs and B cells. Similar to human PCs, cell surface BCMA expression was detected on cynomolgus monkey BM-derived PCs but not on BM-derived B cells (Figure 4A-B; supplemental Figure 3C-D). Despite reports of BCMA protein expression on B cells from cynomolgus monkey peripheral blood (PB),[26] BCMA protein was not detected on B cells or B-cell subsets from cynomolgus monkey PB (Figure 4C; gating strategy in supplemental Figure 3E). BiTE molecules may detect target antigens with higher sensitivity than flow cytometry antibodies. To confirm functionally the lack of BCMA expression on cynomolgus peripheral B cells, AMG 701–mediated T-cell activation and target cell depletion were evaluated in cynomolgus monkey whole blood. Although a tool CD20 BiTE molecule constructed from a published sequence[33] induced T-cell activation and autologous B-cell depletion in cynomolgus monkey whole blood (n = 5), AMG 701 did not induce T-cell activation or B-cell depletion (Figure 4D), functionally corroborating the absence of cell surface BCMA expression. Collectively, these studies confirm the use of cynomolgus monkey as an appropriate preclinical species for the assessment of AMG 701.

Development of a sensitive and quantitative ddPCR-based assay to measure cynomolgus monkey PC-specific gene expression from blood and BM

To measure the in vivo pharmacological activity of AMG 701, we developed a sensitive and quantitative ddPCR-based assay measuring the expression of genes characteristic of PCs. A pure population of cynomolgus monkey PCs was isolated by fluorescence automated cell sorting (97% ± 4% viability, 87% ± 7% purity, n = 4; supplemental Figure 4A) and spiked into PC-depleted BMMC and PBMC samples in increasing numbers, ultimately comprising 0% to 3% of the total cell mixture (supplemental Figure 4B) and representing the physiological range of PC frequency in BM and PB. RNA was isolated from these cell mixtures, and the number of *BCMA* and *J-chain* transcripts (genes reported to be restricted to human PCs[8,26,34]) was quantified by ddPCR (supplemental Figure 4B-C). *BCMA* and *J-chain* transcripts were not detected in PC-depleted BMMC samples (supplemental Figure 4C) or in PC-depleted PBMC samples (data not shown). *BCMA* and *J-chain* messenger RNA (mRNA) detection correlated highly with the number of PCs spiked into PC-depleted BMMC samples (R^2 = +0.9994 and +0.9975, respectively; supplemental Figure 4C). Similar results were observed with PBMC samples. Using this methodology, as few as 1 PC in 1000 PC-depleted BMMCs or PBMCs could be detected (sensitivity, 0.1%), with a dynamic range of 30 (linear dynamic range for ddPCR assays, 0.1%-3% PCs).

To understand the normal variability in *BCMA* and *J-chain* transcript expression over time, a longitudinal study was conducted. The absolute number of *BCMA* and *J-chain* transcripts per nanogram of RNA differed between individuals (supplemental Figure 5); however, for a given individual, *BCMA* and *J-chain* transcript expression was largely stable over time and can be quantified as a reliable biomarker of cynomolgus monkey PCs.

AMG 701–depleted blood and BM PCs in cynomolgus monkeys

In a single-dose study (n = 2 cynomolgus monkeys), AMG 701 exhibited a consistent PK profile (supplemental Figure 6A), with a mean elimination half-life ($t_{1/2}$) ~ 112 hours (4.7 days) (supplemental Figure 6B). AMG 701 was subsequently assessed in a multiple-dose study with 3 dose groups (n = 3 per group) intended to achieve a maximal serum concentration (C_{max}) of 1 nM (group 1), 5 nM (group 2), and 25 nM (group 3) (supplemental Table 3). Exposure of AMG 701 measured as serum concentration over 12 days within each of the 3 groups was reproducible (Figure 5A) and exposure, C_{max}, and minimal serum concentration (C_{min}) all increased in an approximately dose-proportional manner (supplemental Table 3). The $t_{1/2}$ ranged from 66 to 107 hours (supplemental Table 3). At C_{min}, the exposure of AMG 701 was

Figure 3. (continued) middle panel). Forward and side scatter properties of cynomolgus monkey BM PCs (red) backgated onto the singlets (gray, lower right panel). (B) Cell surface flow cytometry analysis of CS1 and CD38 expression on cynomolgus monkey BM PCs (upper panels). Backgating of PCs (red) onto singlets depicting shape, as well as CD27, CS1, and CD138 expression (lower panels). (C) Wright Giemsa staining of a cytospin preparation of flow-sorted cynomolgus monkey PCs from 2 donors. Images taken at original magnification ×100.

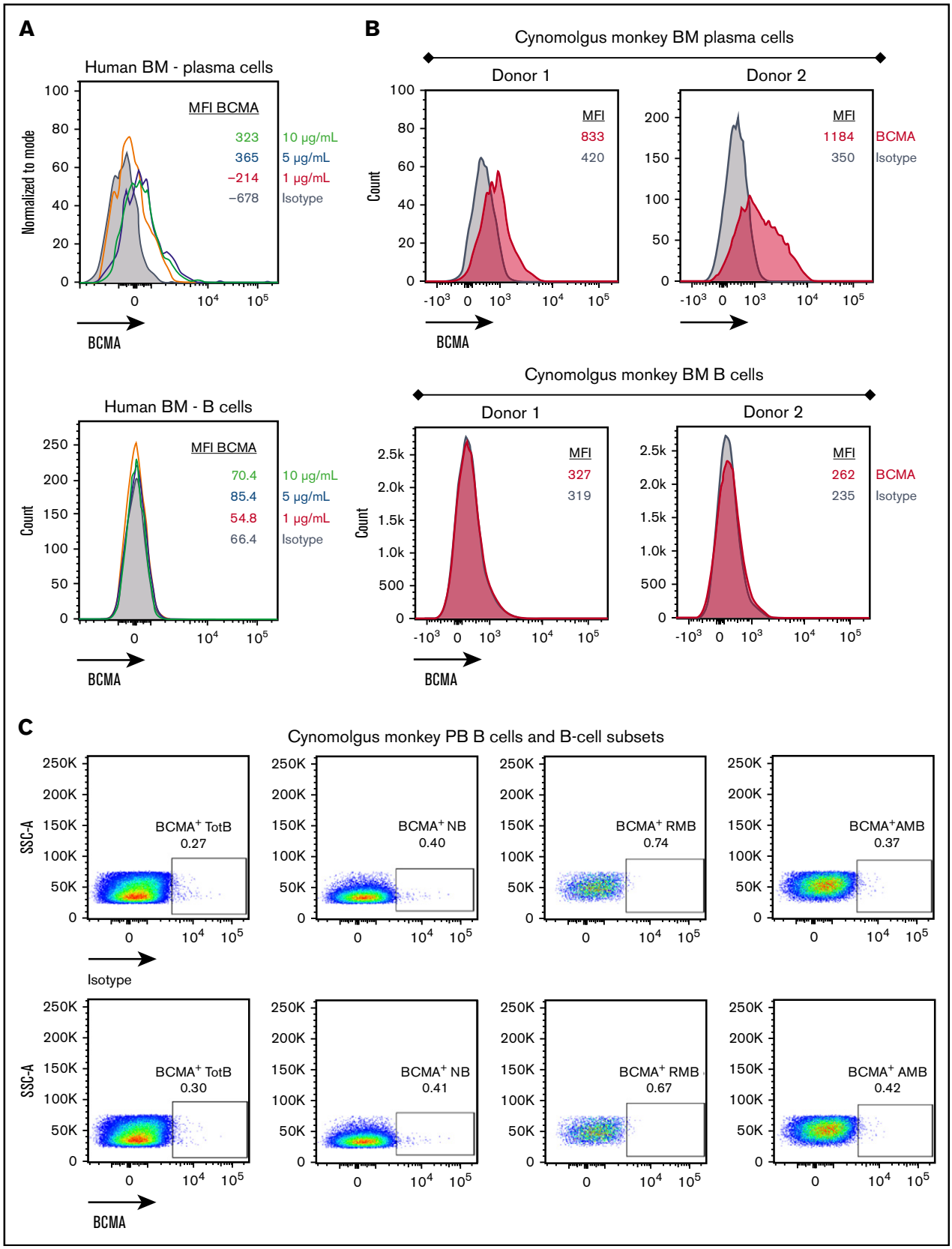

Figure 4. BCMA is expressed on human and cynomolgus monkey BM plasma cells but not on B cells. Flow cytometry histogramsdepicting cell surface BCMA expression levels on plasma cells and CD20^{+} B lineage cells from human (A) and cynomolgus monkey (B) BM. Concentrations of anti-BCMA antibody tested and corresponding mean fluorescence intensity (MFI) values are indicated. (C) Flow cytometry pseudocolor plots representing BCMA expression on cynomolgus monkey PB total B cells

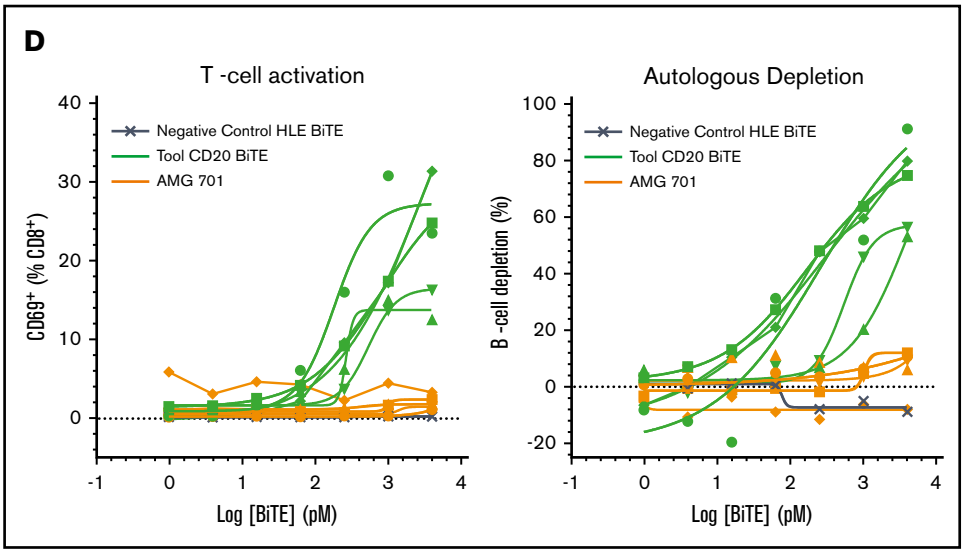

Figure 4. (continued) (TotB), naive B cells (NB), resting memory B cells (RMB), and activated memory B cells (AMB), stained with isotype control (upper panels) or BCMA antibody (lower panels) Plots are representative of 2 donors. (D) T-cell activation shown as $CD69^+$ percentage of $CD8^+$ cells (left panel) and autologous depletion of $CD40^+$ B cells shown as percentage of control (right panel) in cynomolgus monkey whole blood incubated with a negative control HLE BiTE molecule, tool CD20 BiTE molecule, or AMG 701 for 48 hours. Each line represents 1 donor.

sixfold, 20-fold, and 77-fold the in vitro EC_{90} (90% maximal effective concentration, 59 pM) of AMG 701 using cynomolgus monkey effector cells (supplemental Figure 1A; supplemental Table 3). In vivo, AMG 701 induced a dose-dependent depletion of PCs in blood and BM (Figure 5B; supplemental Table 4). Greater depletion of PC genes was observed in blood compared with BM. In BM, PC gene depletion increased with time of exposure, reaching 85% (*BCMA*) and 74% (*J-chain*) on day 12 at the highest dose tested. In blood, depletion of *BCMA* and *J-chain* transcript levels was greater on day 6 than on day 12 (*BCMA* day 6: 72%, 91%, 97% vs day 12: 62%, 70%, 93%; *J-chain* day 6: 66%, 92%, 98% vs day 12: 41%, 71%, 86% for groups 1-3, respectively; average per group, n = 3 per group), with the most sustained depletion observed at the highest dose. In blood, the degree of *BCMA* and *J-chain* transcript depletion was similar. In BM, although both genes followed a similar trend, the extent of *BCMA* transcript depletion was greater than *J-chain* transcript depletion. Minimal, yet dose-dependent, T-cell activation (Figure 5C) and cytokine secretion (Figure 5D) were observed, likely due to the restricted expression of BCMA protein. AMG 701 was well tolerated, as evidenced by stable body weight and temperature.

AMG 701 induced PD-1 expression on T cells and combination with PD-1–blocking antibody increased its potency in vitro

PD-1 expression is induced on T cells upon T-cell activation, and binding of PD-1 to its ligands PD-L1 or PD-L2 decreases T-cell activity.[35] Likewise, AMG 701–mediated T-cell activation induced a dose-dependent increase in PD-1 expression on T cells (Figure 6A). The timing, magnitude, and duration of PD-1 induction varied with different E:T ratios (Figure 6A). In assays with lower E:T ratios, most T cells were $PD\text{-}1^+$, and expression was maintained for a longer time compared with assays with higher E:T ratios. The impact of PD-1/PD-L1 engagement[36,37] on the potency of AMG 701 was assessed. In cocultures of $PD\text{-}1^+$ T cells (supplemental Figure 7A) with PD-L1–overexpressing MM cell lines, AMG 701 potency was reduced three- to fourfold compared with vector-transduced cells (supplemental Figure 7B). Addition of a PD-1–blocking antibody resulted in statistically significant (four- and fivefold) increases in AMG 701 potency ($P = .01$, $P = .0008$, paired Student *t* test; n = 5 pan T-cell donors; Figure 6B-C) and maximum killing ($P = .0096$, $P = .002$; supplemental Figure 7C). In an assay designed to more closely represent a normal physiologic state, using $PD\text{-}1^-$ T cells, the addition of a PD-1–blocking antibody increased AMG 701 potency three- and twofold (Figure 6D). Increased cytotoxicity was associated with increased secretion of interferon-γ and tumor necrosis factor-α (Figure 6E; supplemental Figure 7D).

Model of AMG 701:BCMA interaction has implications for BiTE molecule mechanism of action

To understand the molecular mechanism of action of AMG 701, a model depicting AMG 701 recognition of BCMA and CD3 was constructed based on the crystal structure of the complex of OKT3 Fab with CD3γε (PDB:1SY6). The anti-BCMA scFv was docked to BCMA (PDB:1XU2) based on epitope information detailed in patent US10072088. The 3-dimensional model suggests that AMG 701 can form an immunological synapse with an approximate distance of 100 Å from the tumor cell membrane to the T-cell membrane (Figure 7). This distance is comparable to that generated through the interaction of a TCR with a peptide–major histocompatibility complex class I molecule (pMHC) (TCR:pMHC; PDB: 1BD2). In this model, the half-life–extending Fc moiety does not affect AMG 701 binding of BCMA or CD3 and can be accommodated within the 100-Å synapse. These data are consistent with previous reports that BiTE molecules achieve optimal target cell killing by mimicking the TCR:pMHC immunological synapse.

Discussion

With no curative therapies and ~50% survival 5 years after diagnosis,[3] there is an unmet need for novel therapies for MM. Herein, an HLE anti-BCMA BiTE molecule was characterized in preclinical models. BCMA is an ideal target for a BiTE molecule because of the universal and elevated expression on MM cells and normal expression restricted to PCs.[8] AMG 701 induced specific

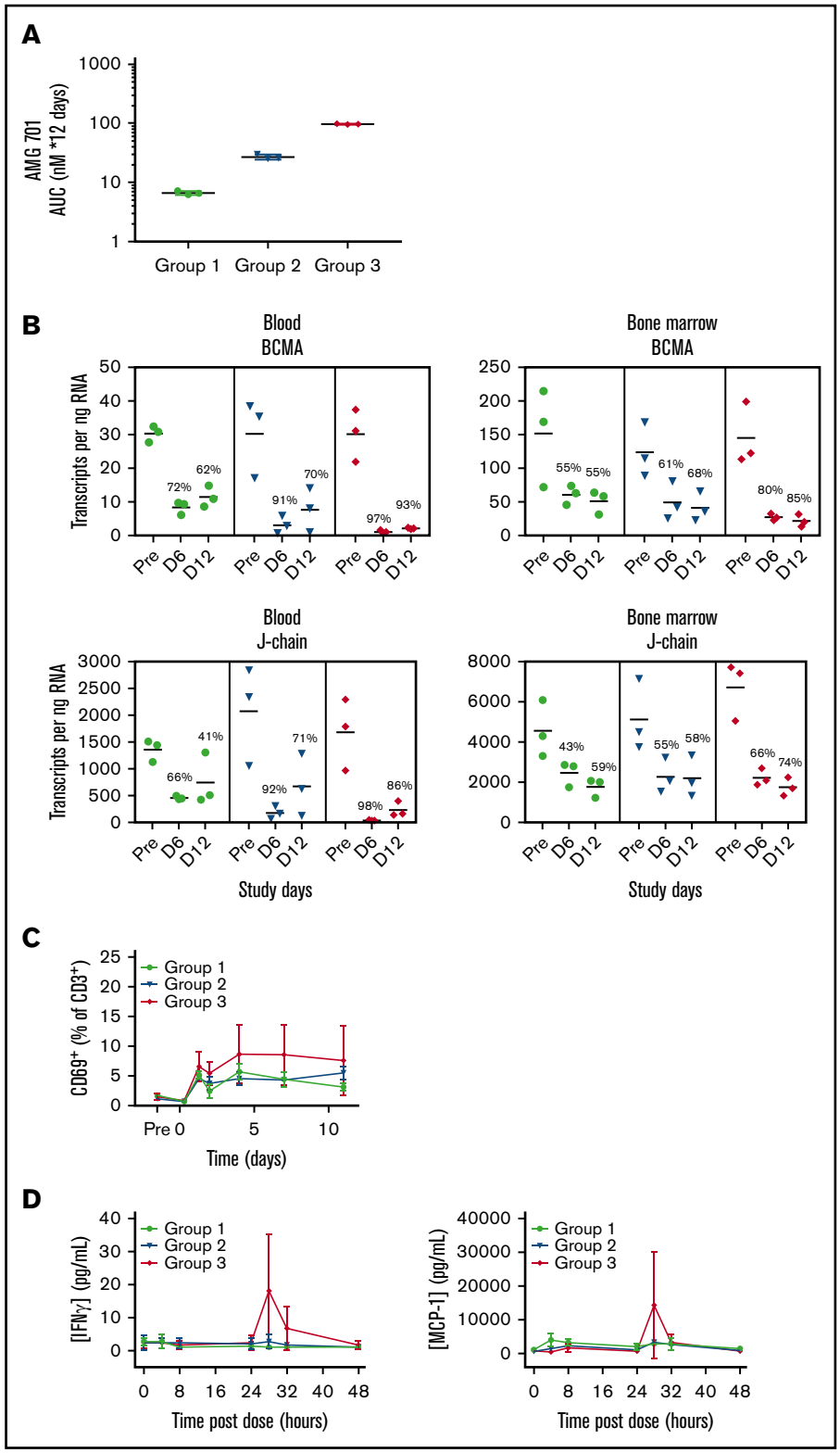

Figure 5. Robust depletion of BCMA mRNA indicates effective AMG 701–mediated elimination of BCMA$^+$ cells in blood and BM of cynomolgus monkeys in vivo. (A) Mean (± standard deviation) exposure of AMG 701 in cynomolgus monkeys (n = 3 per group), represented as area under the concentration-time curve (AUC), calculated as nanomolar AMG 701 administered per day times 12 days of administration. (B) Absolute number of *BCMA* and *J-chain* mRNA transcripts in blood and BM per nanogram of RNA quantified by ddPCR predose (Pre) and on days 6 (D 6) and day 12 (D 12) postdose in cynomolgus monkeys, treated as in panel A. Numbers indicate mean percentage of depletion relative to predose. T-cell activation shown as CD69$^+$ percentage of CD3$^+$ cells (C) and serum concentration of interferon-γ (IFNγ; left panel) and MCP-1 (right panel) (D) over time in cynomolgus monkeys, treated as in panel A.

TDCC in vitro against BCMA-expressing MM cell lines with picomolar potency; induced T-cell activation and cytokine release, consistent with the BiTE molecule mechanism of action; inhibited growth of established tumor xenografts; and increased survival in an orthotopic mouse xenograft model.

In vivo assessment of AMG 701 required defining a PC cell surface immunophenotype and BCMA-expression profiling in cynomolgus monkeys. Using known human PC markers, we defined a novel cynomolgus monkey PC cell surface immunophenotype, CD3$^-$ CD20$^-$CD27$^-$CD38^{hi}CS1^{hi}, which was confirmed by cytospin and

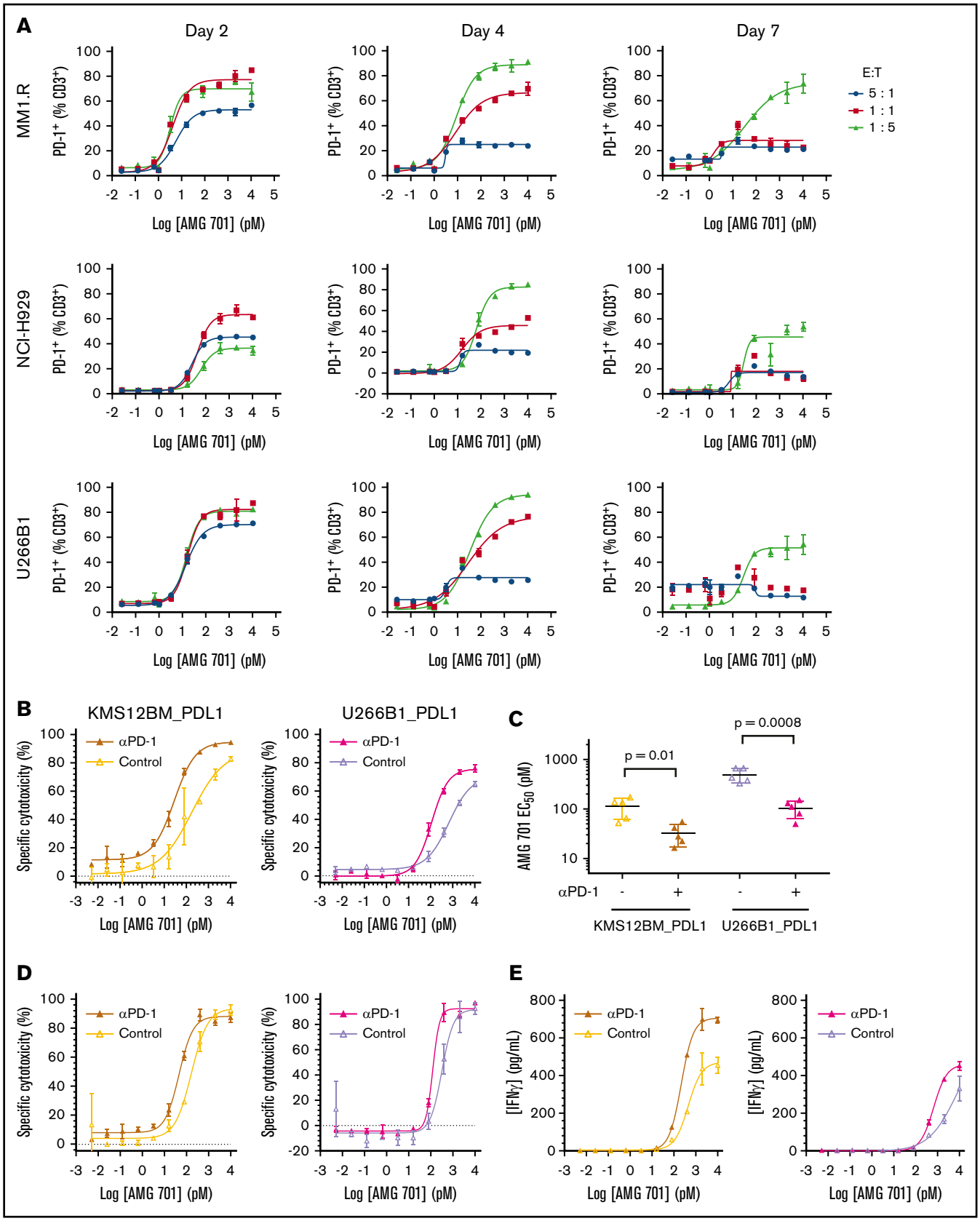

Figure 6. Combination with as PD-1–blocking antibody increases AMG 701 cytotoxicity in vitro. (A) Expression of PD-1 on CD3$^+$ T cells from TDCC assays with cell lines and E:T ratios as indicated, assessed by flow cytometry at different times. Data are mean ± standard deviation (SD) of 2 technical replicates. Curves are

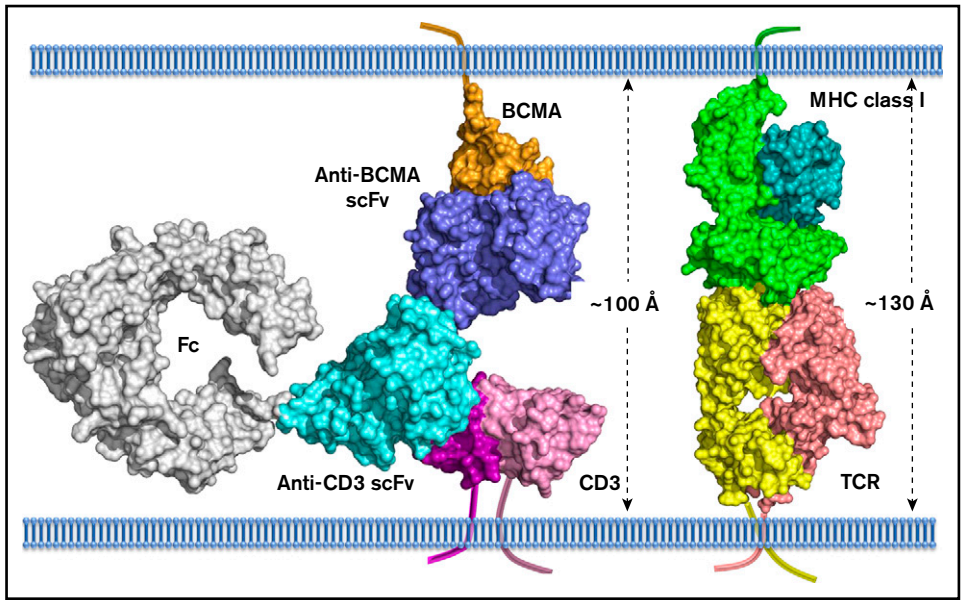

Figure 7. Computational model of extracellular BCMA domain in complex with AMG 701. All proteins are shown in surface representation. BCMA, orange; CD3, magenta and pink; anti-BCMA scFv, blue; anti-CD3 scFv, cyan; Fc, gray; MHC class I, dark cyan and light green; TCR, yellow and salmon. The transmembrane anchor is shown as a ribbon.

Wright Giemsa analysis of sorted cells. In rhesus macaques, a nonhuman primate species commonly used to evaluate human vaccines, characterization of BM and PB PCs identified a population of $CD3^{-}CD19^{+}CD20^{-}CD38^{++}CD138^{++}$ cells with intracellular IgG and variable CD27 expression.[38,39] Despite some similarities in cynomolgus monkey and rhesus macaque PC immunophenotypes, species-specific biology likely exists, given the differences in CD38, CS1, CD138, and CD27 expression. Taken together, we report a novel cynomolgus monkey PC immunophenotype ($CD3^{-}CD20^{-}CD27^{-}CD38^{hi}CS1^{hi}$) and confirm BCMA protein expression on these cells. In contrast with reports in the literature,[26] BCMA was not detected on cynomolgus monkey PB B cells.

Precise quantitation of PCs in BM and blood (frequency, 0.1%-3%) using traditional methodologies, such as cytological evaluation or flow cytometry, is challenging. Therefore, a quantitative ddPCR assay using 2 PC-specific genes, *BCMA* and *J-chain*, was developed to measure AMG 701–induced PC depletion in cynomolgus monkeys. PC depletion in blood and BM was dose-dependent, suggesting increased in vivo activity with increasing exposures. For each dose level, PC depletion was greater in blood than in BM, likely as a result of increased BiTE molecule biodistribution in the blood.[40] Biodistribution of HLE BiTE molecules is similar to monoclonal antibodies, which can demonstrate up to fivefold lower exposure in BM relative to blood.[40-42] Greater depletion of *BCMA* transcripts relative to *J-chain* transcripts observed in BM may reflect the presence of B-cell progenitor cells that express *J-chain*, but not *BCMA*, mRNA.[43] The increased *BCMA* transcript observed at day 12 was not due to loss of exposure but may reflect mobilization of PC precursors that express *BCMA* transcripts but lack BCMA surface protein.[26]

Expression of immune checkpoints that attenuate T-cell activity[35] can be induced by BiTE molecules.[44-46] Likewise, AMG 701–mediated T-cell activation induced PD-1 expression. In TDCC assays of $PD\text{-}1^{+}$ T cells and PD-L1–overexpressing target cells, AMG 701 potency was reduced. The addition of a PD-1–blocking antibody restored AMG 701 potency, consistent with reports of PD-1 blockade with other T-cell–engaging therapeutics.[27,45-47] Further, increased TDCC was observed in the more physiologic context of resting T cells, suggesting that AMG 701–induced PD-1 expression can be targeted by a PD-1–blocking antibody. Increased cytotoxicity was associated with increased cytokine secretion, consistent with the mechanism of action of PD-1 blockade.[48] In MM patients treated with dexamethasone and an immunomodulatory drug, addition of an anti–PD-1 antibody led to increased toxicity,[49] potentially as a result of increased immune activation. In contrast to immunomodulatory drug–induced nonspecific immune activation, BiTE molecules specifically redirect T cells to target-expressing cells. Because of this difference in mechanism and the restricted expression of BCMA, the safety profile of AMG 701, in combination with PD-1 blockade, may be acceptable.

A model of AMG 701 binding to BCMA and CD3 was constructed, and the size of the cytolytic immunological synapse was compared

Figure 6. (continued) representative of 2 human pan T-cell donors. (B) Specific cytotoxicity against KMS12BM_PDL1 (left panel) and U266B1_PDL1 (right panel) cultured for 24 hours 1:1 with CD3/CD28-activated human pan T cells and increasing concentrations of AMG 701, with (closed triangles with dark-shaded curves; mustard or magenta) or without (open triangles with light-shaded curves; yellow or lavender) 10 μg/mL PD-1–blocking antibody. Data are mean ± SD of 2 technical replicates. Curves are representative of 5 pan T-cell donors. (C) EC_{50} of AMG 701, with or without anti–PD-1–blocking antibody, calculated in panel B, n = 5 T-cell donors, KMS12BM_PDL1 (P = .01); U266B1_PDL1 (P = .0008); paired Student t test. Data are mean ± SD. (D) Specific cytotoxicity against KMS12BM_PDL1 and U266B1_PDL1 cultured for 96 hours at 1:5 E:T ratio with resting T cells and increasing concentrations of AMG 701, with (closed triangles with dark-shaded curves; mustard or magenta) or without (open triangles with light-shaded curves; yellow or lavender) 10 μg/mL PD-1–blocking antibody. Data are mean ± SD of 2 technical replicates, representing 1 of 2 assays. (E) Concentration of IFN-γ in supernatants collected from panel D at 72 hours, quantified by an enzyme-linked immunosorbent assay.

with the size of the immunological synapse generated from the interaction of a TCR with MHC class I. BiTE molecules have been previously reported to induce the formation of synapses that are nearly indistinguishable from those formed by TCR:pMHC interaction.[50] We confirmed that the inclusion of the half-life extending Fc domain is not expected to disrupt the size of the synapse. Indeed, AMG 701 potency was similar to the non–Fc-containing anti-BCMA BiTE molecule AMG 420,[20] which has shown a response rate of 70% (7/10) in MM patients at the maximum tolerated dose of 400 μg/d.[22]

Collectively, our preclinical data support the clinical development of AMG 701 in MM patients. Currently, AMG 701 is being examined in a phase 1 FIH clinical study in relapsed/refractory MM patients (NCT03287908).

Acknowledgments

The authors thank Elizabeth Leight (Amgen Inc.) for providing medical writing support and Edward Kim for generating the KMS12BM_PDL1 and U266B1_PDL1 cell lines.

This work was supported by Amgen Inc.

Authorship

Contribution: R.L.G., A.G., C.-M.L., P.D., P.B., O.T., M.K., M. Friedrich, B.R., A.C., M.B., and T.A. contributed to the conception and design of the study; R.L.G., A.G., C.-M.L., P.D., P.B., A. Sternjak, O.T., M.K., J.W., M. Friedrich, E.L., X.M., A. Sudom, and M. Farshbaf conducted experiments; R.L.G., A.G., M.B., and T.A. prepared the manuscript; and all authors analyzed and interpreted the data and read, revised, and approved the final version of the manuscript.

Conflict-of-interest disclosure: R.L.G., C.-M.L., P.D., P.B., A. Sternjak, O.T., M.K., J.W., M. Friedrich, B.R., E.L., X.M., A. Sudom, M. Farshbaf, A.C., and T.A. are employed by Amgen Inc. or Amgen GmbH and are Amgen stockholders. A.G. and M.B. are former employees of Amgen Inc.

The current affiliation for A.G. is Janssen Research and Development, LLC, San Diego, CA.

The current affiliation for M.B. is Biochemical and Cellular Pharmacology, Genentech, South San Francisco, CA.

ORCID profiles: A.G., 0000-0002-6962-727X; C.-M.L., 0000-0002-2740-5652.

Correspondence: Tara Arvedson, Amgen Inc., 1120 Veterans Blvd, South San Francisco, CA 94080; e-mail: taraa@amgen.com; and Mercedesz Balazs, Biochemical and Cellular Pharmacology, Genentech, South San Francisco, CA 94080, e-mail: merci@gene.com.

References

1. Dimopoulos MA, Richardson PG, Moreau P, Anderson KC. Current treatment landscape for relapsed and/or refractory multiple myeloma. *Nat Rev Clin Oncol*. 2015;12(1):42-54.
2. Siegel RL, Miller KD, Jemal A. Cancer Statistics, 2017. *CA Cancer J Clin*. 2017;67(1):7-30.
3. Howlader N, Noone AM, Krapcho M, Miller D, et al In: Cronin KA, eds. SEER Cancer Statistics Review, 1975-2016. Bethesda, MD: National Cancer Institute. (Based on November 2018 SEER data submission, posted to the SEER Web site, April 2019.) https://seercancergov/csr/1975_2016/. Accessed August 2020.
4. Brischwein K, Schlereth B, Guller B, et al. MT110: a novel bispecific single-chain antibody construct with high efficacy in eradicating established tumors. *Mol Immunol*. 2006;43(8):1129-1143.
5. Curran E, Stock W. Taking a "BiTE out of ALL": blinatumomab approval for MRD-positive ALL. *Blood*. 2019;133(16):1715-1719.
6. Stein A, Franklin JL, Chia VM, et al. Benefit-risk assessment of blinatumomab in the treatment of relapsed/refractory B-cell precursor acute lymphoblastic leukemia. *Drug Saf*. 2019;42(5):587-601.
7. Tai YT, Anderson KC. Targeting B-cell maturation antigen in multiple myeloma. *Immunotherapy*. 2015;7(11):1187-1199.
8. Lee L, Bounds D, Paterson J, et al. Evaluation of B cell maturation antigen as a target for antibody drug conjugate mediated cytotoxicity in multiple myeloma. *Br J Haematol*. 2016;174(6):911-922.
9. Tai YT, Mayes PA, Acharya C, et al. Novel anti-B-cell maturation antigen antibody-drug conjugate (GSK2857916) selectively induces killing of multiple myeloma. *Blood*. 2014;123(20):3128-3138.
10. Trudel S, Lendvai N, Popat R, et al. Targeting B-cell maturation antigen with GSK2857916 antibody-drug conjugate in relapsed or refractory multiple myeloma (BMA117159): a dose escalation and expansion phase 1 trial. *Lancet Oncol*. 2018;19(12):1641-1653.
11. Trudel S, Lendvai N, Popat R, et al. Antibody-drug conjugate, GSK2857916, in relapsed/refractory multiple myeloma: an update on safety and efficacy from dose expansion phase I study. *Blood Cancer J*. 2019;9(4):37.
12. Kinneer K, Flynn M, Thomas SB, et al. Preclinical assessment of an antibody-PBD conjugate that targets BCMA on multiple myeloma and myeloma progenitor cells. *Leukemia*. 2019;33(3):766-771.
13. Xing L, Lin L, Yu T, et al. A novel BCMA PBD-ADC with ATM/ATR/WEE1 inhibitors or bortezomib induce synergistic lethality in multiple myeloma. *Leukemia*. 2020;34(8):2150-2162.
14. Berdeja JG, Lin Y, Raje NS, et al. First-in-human multicenter study of bb2121 anti-BCMA CAR T-cell therapy for relapsed/refractory multiple myeloma: updated results. *J Clin Oncol*. 2017;35(15 suppl):3010.
15. Cohen AD, Garfall AL, Stadtmauer EA, et al. B-cell maturation antigen (BCMA)-specific chimeric antigen receptor T cells (CART-BCMA) for multiple myeloma (MM): initial safety and efficacy from a phase I study [abstract]. *Blood*. 2016;128(22):Abstract 1147.

16. Raje N, Berdeja J, Lin Y, et al. Anti-BCMA CAR T-cell therapy bb2121 in relapsed or refractory multiple myeloma. *N Engl J Med*. 2019;380(18):1726-1737.

17. Brudno JN, Maric I, Hartman SD, et al. T cells genetically modified to express an anti-B-cell maturation antigen chimeric antigen receptor cause remissions of poor-prognosis relapsed multiple myeloma. *J Clin Oncol*. 2018;36(22):2267-2280.

18. Xu J, Chen LJ, Yang SS, et al. Exploratory trial of a biepitopic CAR T-targeting B cell maturation antigen in relapsed/refractory multiple myeloma. *Proc Natl Acad Sci USA*. 2019;116(19):9543-9551.

19. Cohen AD, Garfall AL, Stadtmauer EA, et al. B cell maturation antigen-specific CAR T cells are clinically active in multiple myeloma. *J Clin Invest*. 2019;129(6):2210-2221.

20. Hipp S, Tai YT, Blanset D, et al. A novel BCMA/CD3 bispecific T-cell engager for the treatment of multiple myeloma induces selective lysis in vitro and in vivo [published correction appears in *Leukemia*. 2017;31(10):2278]. *Leukemia*. 2017;31(8):1743-1751.

21. Panowski SH, Kuo TC, Zhang Y, et al. Preclinical efficacy and safety comparison of CD3 bispecific and ADC modalities targeting BCMA for the treatment of multiple myeloma. *Mol Cancer Ther*. 2019;18(11):2008-2020.

22. Topp MS, Duell J, Zugmaier G, et al. Anti-B-cell maturation antigen BiTE molecule AMG 420 induces responses in multiple myeloma. *J Clin Oncol*. 2020;38(8):775-783.

23. Carter CM, Cregar LC, Aulbach AD. Cytological bone marrow cell differential counts and morphologic findings in healthy cynomolgus monkeys (*Macaca fascicularis*) from nonclinical toxicology studies. *Toxicol Pathol*. 2017;45(2):267-274.

24. Groves CJ, Carrell J, Grady R, et al. CD19-positive antibody-secreting cells provide immune memory. *Blood Adv*. 2018;2(22):3163-3176.

25. Mei HE, Yoshida T, Sime W, et al. Blood-borne human plasma cells in steady state are derived from mucosal immune responses. *Blood*. 2009;113(11):2461-2469.

26. Seckinger A, Delgado JA, Moser S, et al. Target expression, generation, preclinical activity, and pharmacokinetics of the BCMA-T cell bispecific antibody EM801 for multiple myeloma treatment. *Cancer Cell*. 2017;31(3):396-410.

27. Li J, Stagg NJ, Johnston J, et al. Membrane-proximal epitope facilitates efficient T cell synapse formation by anti-FcRH5/CD3 and is a requirement for myeloma cell killing. *Cancer Cell*. 2017;31(3):383-395.

28. Terstappen LW, Johnsen S, Segers-Nolten IM, Loken MR. Identification and characterization of plasma cells in normal human bone marrow by high-resolution flow cytometry. *Blood*. 1990;76(9):1739-1747.

29. Jourdan M, Caraux A, Caron G, et al. Characterization of a transitional preplasmablast population in the process of human B cell to plasma cell differentiation. *J Immunol*. 2011;187(8):3931-3941.

30. Avery DT, Ellyard JI, Mackay F, Corcoran LM, Hodgkin PD, Tangye SG. Increased expression of CD27 on activated human memory B cells correlates with their commitment to the plasma cell lineage. *J Immunol*. 2005;174(7):4034-4042.

31. Muccio VE, Saraci E, Gilestro M, et al. Multiple myeloma: new surface antigens for the characterization of plasma cells in the era of novel agents. *Cytometry B Clin Cytom*. 2016;90(1):81-90.

32. Caraux A, Klein B, Paiva B, et al; Myeloma Stem Cell Network. Circulating human B and plasma cells. Age-associated changes in counts and detailed characterization of circulating normal CD138− and CD138+ plasma cells. *Haematologica*. 2010;95(6):1016-1020.

33. Mössner E, Brünker P, Moser S, et al. Increasing the efficacy of CD20 antibody therapy through the engineering of a new type II anti-CD20 antibody with enhanced direct and immune effector cell-mediated B-cell cytotoxicity. *Blood*. 2010;115(22):4393-4402.

34. Castro CD, Flajnik MF. Putting J chain back on the map: how might its expression define plasma cell development? *J Immunol*. 2014;193(7):3248-3255.

35. Carter L, Fouser LA, Jussif J, et al. PD-1:PD-L inhibitory pathway affects both CD4(+) and CD8(+) T cells and is overcome by IL-2. *Eur J Immunol*. 2002;32(3):634-643.

36. LaFleur MW, Muroyama Y, Drake CG, Sharpe AH. Inhibitors of the PD-1 pathway in tumor therapy. *J Immunol*. 2018;200(2):375-383.

37. Sharpe AH, Pauken KE. The diverse functions of the PD1 inhibitory pathway. *Nat Rev Immunol*. 2018;18(3):153-167.

38. Demberg T, Brocca-Cofano E, Xiao P, et al. Dynamics of memory B-cell populations in blood, lymph nodes, and bone marrow during antiretroviral therapy and envelope boosting in simian immunodeficiency virus SIVmac251-infected rhesus macaques. *J Virol*. 2012;86(23):12591-12604.

39. Neumann B, Klippert A, Raue K, Sopper S, Stahl-Hennig C. Characterization of B and plasma cells in blood, bone marrow, and secondary lymphoid organs of rhesus macaques by multicolor flow cytometry. *J Leukoc Biol*. 2015;97(1):19-30.

40. Tabrizi M, Bornstein GG, Suria H. Biodistribution mechanisms of therapeutic monoclonal antibodies in health and disease. *AAPS J*. 2010;12(1):33-43.

41. Baxter LT, Zhu H, Mackensen DG, Butler WF, Jain RK. Biodistribution of monoclonal antibodies: scale-up from mouse to human using a physiologically based pharmacokinetic model. *Cancer Res*. 1995;55(20):4611-4622.

42. Matesan MC, Fisher DR, Wong R, et al. Biokinetics of radiolabeled monoclonal antibody BC8: differences in biodistribution and dosimetry among hematologic malignancies [published online ahead of print 13 March 2020]. *J Nucl Med*. doi:10.2967/jnumed.119.234443

43. Bertrand FE III, Billips LG, Gartland GL, Kubagawa H, Schroeder HW Jr.. The J chain gene is transcribed during B and T lymphopoiesis in humans. *J Immunol*. 1996;156(11):4240-4244.

44. Köhnke T, Krupka C, Tischer J, Knösel T, Subklewe M. Increase of PD-L1 expressing B-precursor ALL cells in a patient resistant to the CD19/CD3-bispecific T cell engager antibody blinatumomab. *J Hematol Oncol*. 2015;8(1):111.

45. Krupka C, Kufer P, Kischel R, et al. Blockade of the PD-1/PD-L1 axis augments lysis of AML cells by the CD33/CD3 BiTE antibody construct AMG 330: reversing a T-cell-induced immune escape mechanism. *Leukemia*. 2016;30(2):484-491.

46. Feucht J, Kayser S, Gorodezki D, et al. T-cell responses against CD19+ pediatric acute lymphoblastic leukemia mediated by bispecific T-cell engager (BiTE) are regulated contrarily by PD-L1 and CD80/CD86 on leukemic blasts. *Oncotarget*. 2016;7(47):76902-76919.

47. Junttila TT, Li J, Johnston J, et al. Antitumor efficacy of a bispecific antibody that targets HER2 and activates T cells. *Cancer Res*. 2014;74(19): 5561-5571.

48. Wei SC, Duffy CR, Allison JP. Fundamental mechanisms of immune checkpoint blockade therapy. *Cancer Discov*. 2018;8(9):1069-1086.

49. Mateos MV, Blacklock H, Schjesvold F, et al; KEYNOTE-183 Investigators. Pembrolizumab plus pomalidomide and dexamethasone for patients with relapsed or refractory multiple myeloma (KEYNOTE-183): a randomised, open-label, phase 3 trial. *Lancet Haematol*. 2019;6(9):e459-e469.

50. Offner S, Hofmeister R, Romaniuk A, Kufer P, Baeuerle PA. Induction of regular cytolytic T cell synapses by bispecific single-chain antibody constructs on MHC class I-negative tumor cells. *Mol Immunol*. 2006;43(6):763-771.